

Discharge hydrograph and flow depths for a post-wildfire sediment-laden flood in a small watershed near Monte Lake

Kaushal Gnyawali, M.Eng.^{1,2}, Dwayne Tannant, Ph.D¹, Tom Millard, M.Sc.², Brendan Miller, M.Sc.², Sarah Crookshanks, M.Sc.²

¹School of Engineering, University of British Columbia Okanagan, Kelowna, B.C., Canada;
e-mail: dwayne.tannant@ubc.ca

²B.C. Ministry of Forests, B.C., Canada

ABSTRACT

A post-wildfire sediment-laden flood affected a small watershed fan apex in south-central British Columbia. We estimate the discharge hydrograph, then using Newtonian flow assumptions, simulate the sediment-laden flow height and velocity on a high-resolution fan topography. Post-event field observations and video records of flow during the event are used to calibrate an integrated HEC-HMS and HEC-RAS model. The paper demonstrates a workflow to simulate post-wildfire sediment-laden floods in small watersheds.

INTRODUCTION

Post-wildfire sediment-laden floods in small watersheds are poorly documented events. The engineering parameters required to design structures to mitigate damage, like discharge, sediment yield, and flow velocities, are challenging to predict. Existing empirical equations are biased towards larger watersheds and grossly overestimate discharge and sediment yield in small watersheds in south-central British Columbia (B.C.). Developing a workflow to correctly estimate the discharge, velocity, sediment yield, and flow height of sediment-laden floods in small watersheds of B.C. is crucial to appropriately design and install terrain-based mitigations like deflection berms and ditches at appropriate locations in the fan to mitigate the risk of sediment-laden flood hazards. This research builds resiliency in response to climate change and the increasing occurrence of wildfires in the region in the long term.

This paper documents post-event field observations of a sediment-laden flood in the Monte Lake area of B.C. on June 28, 2022, in response to a localized convective storm. This area was burned by the White Rock Lake fire in the summer of 2021. Visual observations of flow height, wetted channel width, and erosion depth were documented at two locations in the watershed. Video records made during the flow were used to constrain the discharge and velocity. An HEC-HMS model was developed to predict the discharge hydrograph at the fan of the small watershed. The discharge hydrograph was then fed into an HEC-RAS model to predict the flow heights and velocities at different locations of the alluvial fan at the base of the small watershed using a high-resolution topographic model.

SMALL WATERSHED OVERVIEW

The small watershed has an area of 0.28 km² with a relative relief of 408 m. It lies in south-central B.C. near Monte Lake at 50°30'9.01 "N and 119°49'50.72"W. Figure 1 shows the watershed topography. The slopes face west. The watershed lies within the Interior Douglas-fir zone (BCMFR 2007). The dominant soil type is sandy silt with some organic carbon content.

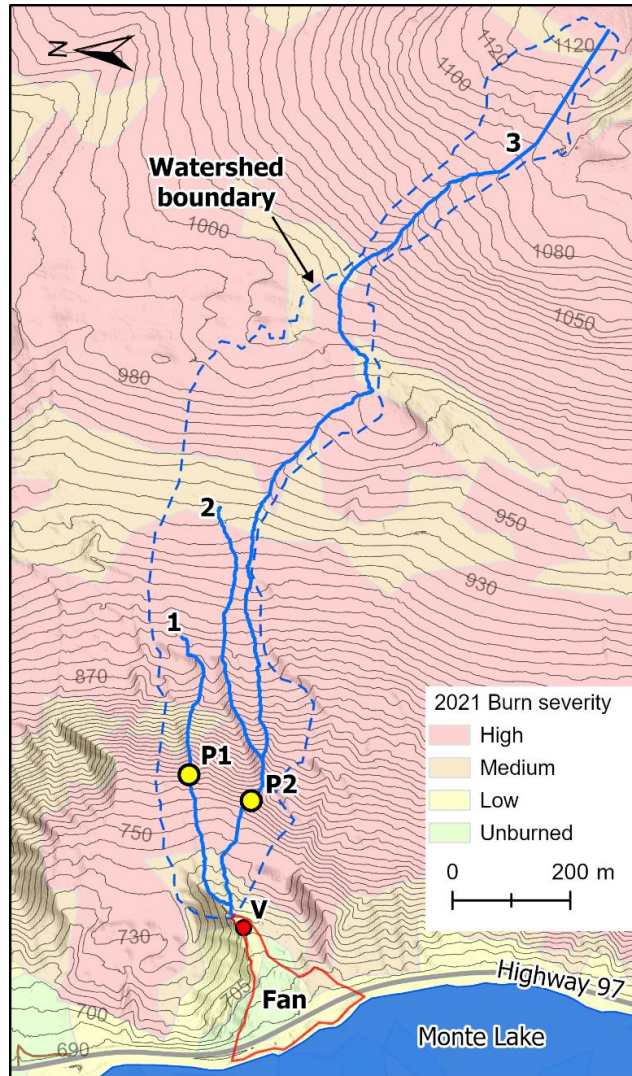


Figure 1 Topographic map showing watershed boundary, ephemeral channels (1-3), alluvial fan, and overlaid on the 2021 wildfire burn severity map. P1 and P2 correspond to locations where flood heights and velocities were estimated from field observations. V corresponds to the location where a video of the event was taken.

The summertime convective rainfall clouds in the region typically move from the southwest to the northeast. The mean annual temperature and precipitation between 1991 to 2020 were 6.4 °C and 454 mm, respectively. The mean precipitation for June in the mid to upper watersheds near Monte Lake is approximately 60 mm (ClimateBC_Map, 2022) for the same

period. Interpolated historical data of rainfall intensity from the IDF CC tool v6.5 for 15 minutes of rainfall is 5.28 mm (2-year return period), 10.52 mm (10-year return period), 17.42 (50-year return period), and 21.27 (100-year return period) (Simonovic et al., 2015).

Watershed morphometrics

The small watershed has three ephemeral channels (1-3) that merge at the fan apex, Figure 1 Topographic map showing watershed boundary, ephemeral channels (1-3), alluvial fan, and overlaid on the 2021 wildfire burn severity map. P1 and P2 correspond to locations where flood heights and velocities were estimated from field observations. V corresponds to the location where a video of the event was taken. The longest ephemeral channel is 1937 m long, with a relief of 408 m and an average channel gradient of 11.9°. The mean watershed slope is 15°, the mean terrain ruggedness index is 0.2, and the Melton ratio is 0.76. The Melton ratio and the channel length place the watershed in a mixed debris flood and debris flows zone (Church and Jakob, 2020).

Fan morphometrics

The alluvial fan at the base of the watershed is covered by widely spaced mature pine and fir trees and has evidence of old small debris flows. The fan has an area of 0.022 km². Residential homes and recreational vehicles are located on the fan. The fan has an average gradient of 6.9° and a relief of 29 m. The fan is 170 m long and 240 m wide. An ephemeral channel runs along an earth road near the centre of the fan and then crosses Highway 97.

Wildfire effects

The White Rock Lake fire burnt the watershed between August 5 and 8, 2021, and evacuation orders were issued for the Monte Lake area (Little, 2021). By the time of the June 2022 rainfall event, grasses within the burned area had somewhat regenerated. Wildfire likely increases runoff and soil erosion (Hope et al., 2015); however, it is impossible to quantify the wildfire effect's significance for the June 28, 2022 event. Soil water repellency was only infrequently observed in the burned area. Water was also observed in unburned areas. Soil burn severities were generally moderate, with organic matter mostly being consumed. The vegetation on the lower part of the watershed was burnt at medium burn severity, and the upper part was burnt at high burn severity (Figure 1).

Rainfall on June 28, 2022

The total storm precipitation on June 28, 2022, is estimated to be 23 to 38 mm, with most rain falling within 10 minutes around 13:40 PDT. People living on the small alluvial fan described the storm as hail followed by the heaviest rain they had ever seen (Turacato, 2022). The weather radar image in Figure 2 shows a maximum precipitation intensity at 13:40 of between 125-199 mm/h, corresponding to 20 to 33 mm of rain falling within 10 minutes (Environment Canada, 2022). Hail has high reflectivity for radar; therefore, the precipitation value may be overestimated.

The precipitation intensity estimate corresponds to a greater than 100-year rainfall event using the IDF_CC Tool version 6.5 (Simonovic et al., 2015).

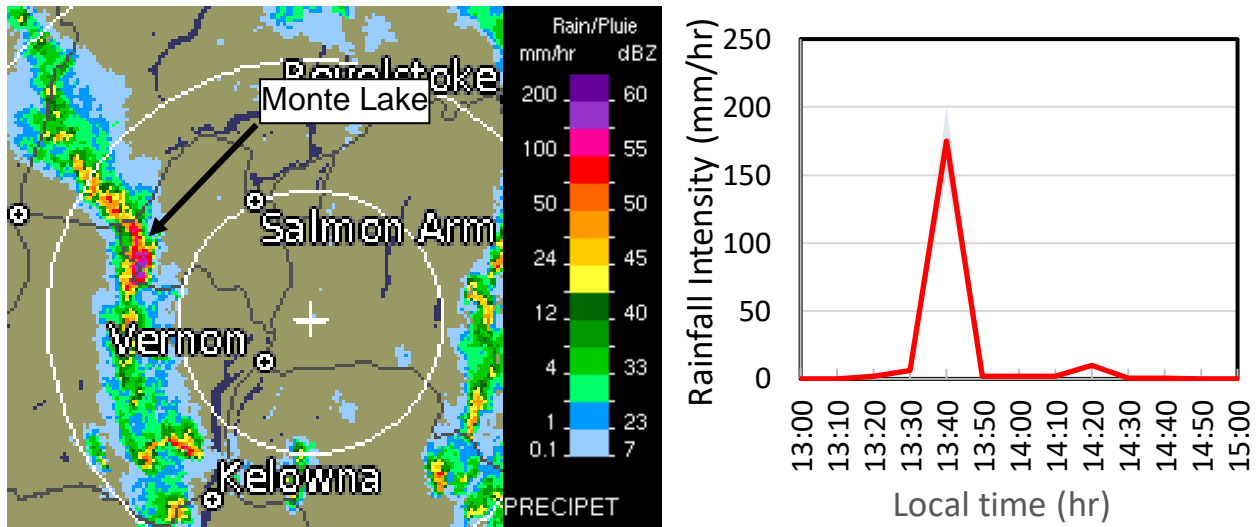


Figure 2 (a) Radar image of the rainfall near Monte Lake on June 28, 2022, at 13:40 PST from Silver Star radar station. (b) Rainfall intensity vs. time recorded at the radar pixel corresponding to the alluvial fan location.

A resident reported the resulting flood as "flowing probably about 10 inches deep down the whole hillside." Another resident reported, "20 minutes of really, really intense rain, and a lot of that came down as hail as well" (Turcato, 2022).

Impact of the sediment-laden flood

The rainfall event caused soil erosion (rilling) within steeper portions of the watershed. Incision within the ephemeral drainage channels was up to 1.5 m deep, causing channel banks to be undercut. The eroded sediment formed a sediment-laden flow, depositing sand, gravel, and burnt woody debris on the fan, covering Highway 97. The drainage channels on the lower part of the fan were choked by debris. Heavy machinery was required to clear the debris from the road and around the houses and trailers located on the fan. The sediment-laden flow across the highway and directly into Monte Lake also impacted a small area between the highway and the lake.

The residents described the event as bigger than anything they had ever seen before and expressed concern that further incidents could arise from that watershed (Turcato, 2022). People were seeking advice on how to protect their homes and infrastructure. Small terrain modifications such as ditches and berms could potentially reduce future impacts.

FIELD MEASUREMENTS AND ANALYSIS

Fieldwork was conducted on July 6, 2022, eight days after the rainfall event. The field measurements are presented later in this paper. The sediment volume deposited on the fan was measured with a tape measure and visual approximation. The wetted width of the channel section

(*B*) during the probable peak discharge was measured at two locations (P1 and P2, Figure 1). The maximum value for *B* was determined by the extent of flattened grass during the flow event. At both locations, the splash height of muddy water on a tree near the channel centre was measured on the front (h_1) and back (h_2), as illustrated in Figure 3.

The flow velocity at each channel section was estimated using two methods, as described in Equations 1 and 2 below. The peak discharge was estimated by multiplying the velocity by the wetted area.

The velocity was estimated using splash height observations and the following equation.

$$v = \sqrt{2 * g * (h_2 - h_1)} \quad (1)$$

where h_2 and h_1 are splash heights observed on the front and back of the tree, respectively, and g is the gravitational acceleration (Chow, 1959).

Chow (1959) assessed the flow velocity in this equation by determining the variation in the run-up (splash) heights on either side of an obstacle in the flow path multiplied by the gravitational constant. This approach has two known drawbacks: first, it only applies to objects located perpendicular to the flow direction, and second, it assumes that all kinetic energy has been transformed into potential energy (Jakob, 2005). Theoretical run-up equations, such as Equation 1, can yield up to 30% lower velocities than those found in flume tests (Jakob, 2005). Nevertheless, the estimated velocity using Equation 1 was not adjusted.

The velocity was also estimated using Manning's equation,

$$v = \frac{R^{2/3} \sqrt{S}}{n} \quad (2)$$

where R is the hydraulic radius, S is the channel gradient (m/m), and n is Manning's roughness coefficient. The selected Manning's n value was relatively high for the flow channels, recognizing shallow flow depth over a rough surface (Table 1).

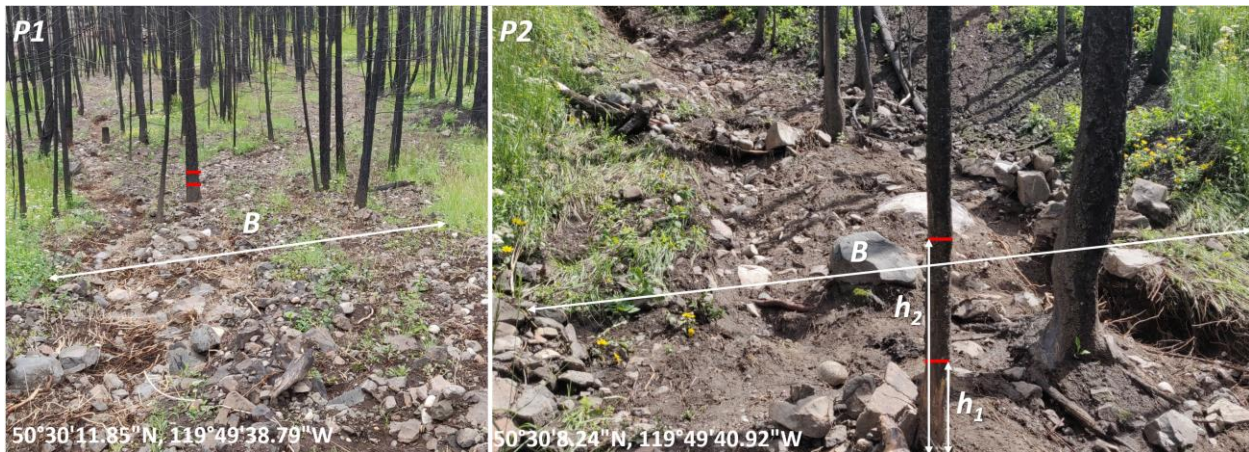


Figure 3 Field measurements taken at two different locations (P1 and P2, in Figure 1): wetted flow width (*B*), splash heights at the front (h_2) and back (h_1) on a tree located near the centre of the channel, and major axis length of the largest clast mobilized (*d*).

Estimate of peak discharge from velocities

The peak flow velocity times the maximum wetted flow cross-section area gives the peak discharge. The wetted flow cross-section is assumed to be rectangular, with the average flow height estimated with a visual interpretation of the channel considering micro-channel undulations. The average flow height was less than the splash height (h_1) at the back of the tree because the tree is located at the deeper section of the wetted channel width. This parameter can be a source of error in further calculations.

Table 1 summarizes the field measurements, flow velocity, and discharge estimates at P1 and P2.

Table 1 Measured and estimated flow parameters.

Description	P1	P2
Flow type	Unconfined	Partially confined
Splash height at the front of the tree (h_2)	0.54 m	1.3 m
Splash height at the back of the tree (h_1)	0.25 m	0.3 m
Wetted width (B)	14 m	6 m
Estimated average flow height (assuming a rectangular cross-section)	0.08 m	0.15 m
Flow area	1.12 m ²	0.9 m ²
Channel gradient	27%	45%
Manning's n	0.06	0.07
Velocity from Equation 1	2.4 m/s	4.4 m/s
Velocity from Equation 2	1.6 m/s	2.6 m/s
Peak velocity range	1.6 – 2.4 m/s	2.6 – 4.4 m/s
Peak discharge range	1.8 – 2.7 m ³ /s	2.3 – 4.0 m ³ /s

In summary, the estimated combined peak discharge from P1 and P2 was between 4.1 – 6.7 m³/s. This water later flows over the fan as a sediment-laden flood. However, it is important to understand that this estimate is based on clearwater flow assumptions. The actual flow contains debris, increasing the total flow volume and reducing the flow velocity.

METHODOLOGY FOR FLOW RECONSTRUCTION

The simulation modelling aimed to obtain a map showing flood heights and flow velocities on an alluvial fan, where homes and infrastructure are located. The work requires two steps. First, a flood discharge hydrograph is generated using HEC-HMS with rainfall, topography, and channel hydrology as input. Second, the estimated discharge hydrograph is used as an inflow boundary condition to simulate the flow on the alluvial fan in HEC-RAS. The input for this step is the high-resolution microtopography, including buildings and other flow obstructions and flow parameters. Field estimates of flow velocities are used in both steps to constrain the models. Constraining the model with field estimates of velocities and discharges is an iterative process.

Sediment-laden flood hydrograph from HEC-HMS

A discharge hydrograph on the watershed outlet at the apex of the fan was estimated using HEC-HMS. The watershed boundary, longest ephemeral channel, and digital terrain model are imported into the software. Basin properties are modelled as a single subbasin. The SCS Curve method with curve number 95 was chosen as the loss method, and the transform method was the SCS unit hydrograph (standard PRF 484 graph type with a lag time of 14 minutes). A Munkingham-Cunge routing method is used. The rainfall was input as time series estimated from historical radar data on June 28, 2022 (Figure 2). A sensitivity analysis was performed on the model. Erosion was estimated with the USGS Emergency Assessment Debris Model (Gartner et al., 2014). The burn area was taken from the burn severity map (Figure 2). The model generates a clearwater flood discharge hydrograph at the apex of the alluvial fan.

Sediment-laden flood flow simulation with HEC-RAS

A HEC-RAS model was created with a 0.25-metre resolution of the fan area. The upstream boundary condition was the discharge hydrograph generated from HEC-RAS. The discharge hydrograph brings the flow into the fan topography. It was released at the fan apex with a cross-section length of 13 m (roughly equal to the wetted channel width at that location) and an energy slope value of 0.13. The energy slope is used to compute a normal depth from the given discharge and the cross-section data (underlying terrain data) along the boundary condition line for each computational time step. Normal depth is the depth corresponding to uniform flow (Chow, 1959). The channel bed slope is equal to the energy slope for normal depth. The energy slope at the upstream boundary condition was measured from the high-resolution terrain model. The downstream boundary condition was taken as a normal flow depth assumption with a friction slope of 0.01. This means the flow exits the downstream boundary (near the highway centreline on nearly flat ground) as a normal flow (uniform flow). The friction slope (S in Manning's Equation 2) is the slope of the energy grade line. It is important to note that the energy slope (at the upstream cross-section) represents the total energy loss from one cross-section to the next and includes the friction losses plus losses from contraction and expansion, while the friction slope is strictly from losses due to roughness. Via iterative simulations, it was found that a Manning's roughness coefficient of 0.18 was required for the model to generate realistic flow depths and velocities on the fan. This value is significantly larger than those estimated for the channels in Figure 3 because it is tied to the numerical stability of the model and adjusted with an iterative trial-and-error approach.

HEC-RAS has three equation sets that can be used to solve for the flow moving over the computational mesh. In this case, two-dimensional unsteady flow routing was chosen with the Shallow Water Equations, Eulerian-Lagrangian Method (SWE-ELM). This method is chosen because it considers changes in velocity with respect to time and distance terms. The time step is adjusted based on the Courant condition (maximum = 3 and minimum = 0.5). The predicted hydrograph at the highway location was compared with the input hydrograph at the fan apex to check the consistency of the results.

RESULTS AND DISCUSSION

Sediment-laden flood hydrograph from HEC-HMS

The predicted flow hydrograph at the fan apex for clearwater flow is the blue line in Figure 4. The peak flow was 4.4 m³/s, and the flow lasted for a little over an hour. The area under the flow hydrograph is the total volume of flow. The total volume of clearwater flood water (V_{water}) from the ephemeral channels estimated from the HEC-HMS model was approximately 6000 m³.

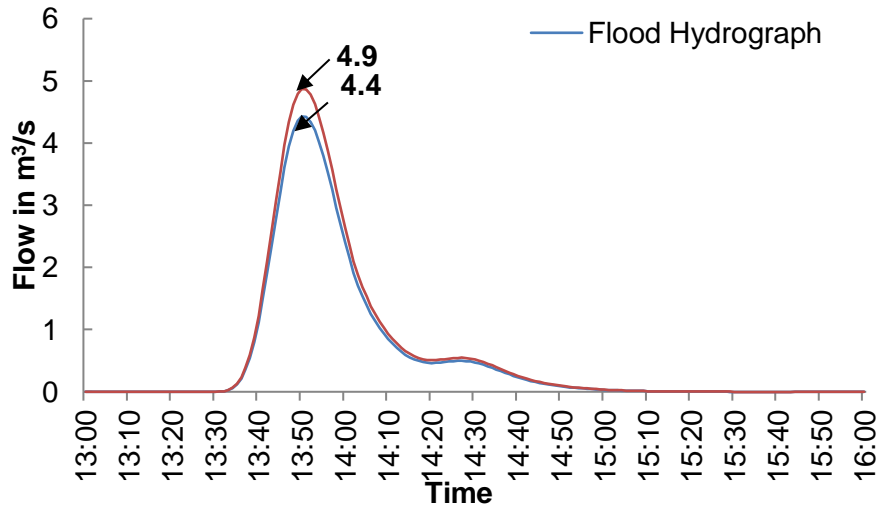


Figure 4 Discharge hydrograph at the fan apex modelled from HEC-HMS redo red line

The actual flow also contained solids in the form of fine gravel, sand, silt, and burnt woody debris. It is essential to know the sediment concentration in the flow to quantify the total volume of water and solids. The sediment concentration, C_v , is given by

$$C_v = V_{sed} / (V_{water} + V_{sed}) \quad (4)$$

where the volume of sediment deposited on the fan (V_{sed}) was estimated to be between 200 and 500 m³. Some fine sediment could have gotten into the lake with the floodwater, and it's volume couldn't be quantified. Therefore, $C_v = 3\%$ to 8% , depending on the actual observed volume of deposited sediment. The sediment concentration allows us to bulk the clearwater flow discharge using a bulking factor, BF , defined as

$$BF = \frac{1}{1 - \frac{C_v}{100}} \quad (5)$$

The red line in Figure 4 shows the bulked hydrograph.

The sediment concentration was independently estimated by interpreting a video record of the flood taken at the approximate time of the peak flow and classifying it according to (Jakob et al., 2022). A video recording was taken on the fan at location V in Figure 1. From visual observations, the flow appeared to contain fine soil and burnt woody debris with a typical sediment concentration of approximately 10%. These flow characteristics are compatible with a Type 1 meteorologically generated debris flood category as defined by (Church and Jakob, 2020; Jakob

et al., 2022). This sediment concentration is consistent with our estimated volume for clearwater discharge and deposited sediment.

A discharge bulking factor of 1.1 was applied to the clearwater hydrograph to create the red line in Figure 4 for the sediment-laden flood discharge hydrograph. The total modelled peak discharge of the sediment-laden flood after bulking was 4.9 m³/s. This modelled peak discharge lies within the range of 4.1 to 6.7 m³/s, determined from field measurements and analysis as presented in Table 1.

We also estimated the sediment USGS Emergency Assessment Debris Model, which accounts for watershed relief, burn area, and rainfall intensity as defined in (Gartner et al., 2014). It estimated the debris volume to be about 6000 m³, which grossly over-predicts the observed debris volume of 200-500 m³ on the fan. This illustrates the limitation of empirical equations embedded in tools like the USGS Emergency Assessment Debris Model. Better relationships are needed for small watersheds affected by wildfires. For further analysis, we simply used the bulked sediment-laden flood hydrograph (Figure 4) as a flow input to the apex of the alluvial fan in an HEC-RAS model.

Flow height and velocity from HEC-RAS

A hydrodynamic model of the alluvial fan was created in HEC-RAS. The topography was derived from a lidar point cloud and resampled at 0.25 m pixel resolution to capture the microtopography. Buildings were incorporated into the microtopography and acted as flow barriers. Figure 5 Modelled flow heights and flow velocities from the HEC-RAS Newtonian model. The map shows the modelled sediment-laden flood's maximum flow height and maximum velocity at different locations. A 2D Newtonian model was chosen to model the flood because the sediment concentration was low. The modelled flow height and velocity were consistent with the video record of the flow taken at location V.

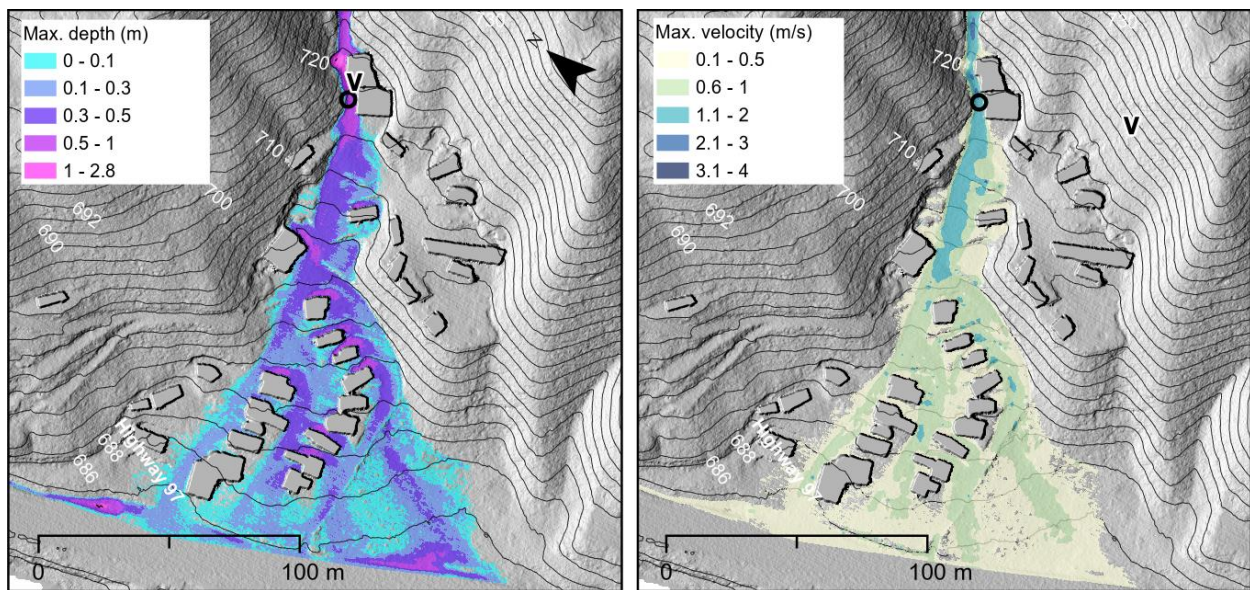


Figure 5 Modelled flow heights and flow velocities from the HEC-RAS Newtonian model.

Maps like that shown in Figure 5 would be invaluable for assessing the consequences of post-wildfire sediment-laden floods and can be used to guide mitigation efforts.

CONCLUSION

A workflow is presented to model a discharge hydrograph of a post-wildfire sediment-laden flood in HEC-HMS and simulate flow depths and velocities in HEC-RAS on a small watershed and alluvial fan near Monte Lake. The modelling was calibrated with post-event field observations and video recordings during the event. The simulation results were consistent with the field observations of flow heights and estimated velocities.

This workflow and modelling approach we used can be extended to simulate small-scale terrain-based mitigation structures like deflection berms and ditches in the future. Lessons learned from this work include:

1. Careful field observations and interpretations of flow heights, deposit volumes, video records, lidar data, and radar rainfall records can help constrain the numerical reconstruction of post-wildfire sediment-laden floods.
2. Existing sediment volume estimation equations (Gartner et al., 2014) overestimate the volume of debris deposited on the fan by over an order of magnitude at this site.
3. Newtonian methods of simulation seem suitable for this type of event. Clearwater discharge with large curve numbers and small bulking factors is suitable for generating the runoff discharge hydrographs.
4. A 2D Newtonian method is suitable for sediment-laden flood modelling on micro-topography when using two-dimensional unsteady flow routing with the Shallow Water Equations, Eulerian-Lagrangian Method (SWE-ELM) and a wider range for Courant condition (maximum =3 and minimum = 0.5 in this case).

REFERENCES

- BCMFR. (2007). *Tree Book: Learning to Recognize Trees of British Columbia*. B.C. Ministry of Forests and Range.
<http://www.for.gov.bc.ca/hfd/library/documents/treebook/index.htm>
- Chow, V.T. (1959). *Open Channel Hydraulics*. McGraw Hill, 680 p.
- Church, M., & Jakob, M. (2020). What is a debris flood? *Water Resources Research*, 56(8).
- ClimateBC_Map. (2022). Centre for Forest Conservation Genetics.
<https://climatebc.ca/mapVersion>
- Gartner, J. E., Cannon, S. H., & Santi, P. M. (2014). Empirical models for predicting volumes of sediment deposited by debris flows and sediment-laden floods in the transverse ranges of southern California. *Engineering Geology*, 176, 45–56.
- Hope, G., Jordan, P., Winkler, R., Giles, T., Curran, M., Soneff, K., & Chapman, B. (2015). *Post-wildfire natural hazards risk analysis in British Columbia*. Land Management Handbook 69, Province of B.C., Victoria, B.C.,
www.for.gov.bc.ca/hfd/pubs/Docs/Lmh/LMH69.htm

- Jakob, M. (2005). Debris-flow hazard analysis, Chapter 17, in Jakob, Matthias., and Hungr, Oldrich., eds., Debris Flow Hazards and Related Phenomena: New York, Springer Praxis Books in Geophysical Sciences, p. 411-443.
- Jakob, M., Davidson, S., Bullard, G., Busslinger, M., Collier-Pandya, B., Grover, P., & Lau, C.-A. (2022). Debris-flood hazard assessments in steep streams. *Water Resources Research*, 58(4).
- Little, S. (2021). More anger, frustration from inside devastated White Rock Lake fire zone. Global News. <https://globalnews.ca/news/8096503/white-rock-lake-monte-lake-fire-anger/> Posted on August 8, 2021.
- Environment Canada. (2022). Canadian Historical Weather Radar - Silver Star Mountain (near Vernon). https://climate.weather.gc.ca/radar/index_e.html?site=CASSS
- Simonovic, S.P., A. Schardong, R. Srivastav, and D. Sandink. (2015). IDF_CC Web-based Tool for Updating Intensity-Duration-Frequency Curves to Changing Climate – ver 6.5, Western University Facility for Intelligent Decision Support and Institute for Catastrophic Loss Reduction, open access <https://www.idf-cc-uwo.ca>.
- Turcato, M. (2022). Heavy rain triggers flash flood in wildfire-hit Monte Lake. Global News. <https://globalnews.ca/news/8957588/monte-lake-flash-flood/>. Posted on June 29, 2022.